Proceedings of the 2021 IEEE
International Conference on Robotics and Biomimetics
December 27-31, 2021, Sanya, China

2021 IEEE International Conference on Robotics and Biomimetics (ROBIO) | 978-1-6654-0535-5/21/$31.00 ©2021 IEEE | DOI: 10.1109/ROBIO54168.2021.9739537

Force Sensations of Delayed Telerobotic System with Kalman Filter

Hongbing Li, Xun Nie, Evgeni Magid, and Dingkun Gui

***Abstract*—The transparency of a telerobotic system indicates a measure of how the human feels the remote system. Haptic perception plays a very important role in improving such system transparency. It enables the operator to feel the environment properties, evaluate object structures, and allow him/her to commit appropriate force control actions for safe manipulation. However, the typical approach to acquire remote contact forces is attaching force sensors on slave robot tip. This complicates system structure, makes delayed system unstable and makes the tool bulky. This paper presents formulation and application of an estimation approach based on Kalman filter for control of master slave robots contacting with unknown environment. A Kalman filter based estimator has been designed to estimate the driving current and rotation speed of the joint actuator. The feasibility of using motor current to estimate tool-environment contact forces is explored. Experimental results are presented, which demonstrate stable behavior of the telerobotic system with communication delay contact with remote environment.**

I. Introduction

HAPTIC sensations are essential for many teleoperation tasks. Minimally invasive surgery is an emerging field for such telerobotics systems. Such teleoperated surgical robot systems offer surgeons magnified 3D HD vision, various surgical instruments with better dexterity than human hand and enhanced ergonomics [1]-[3]. However, one current concern is the lack of force feedback or haptic (touch) sensation available to the surgeon for safe tissue manipulation, making it possible for a surgeon to cause tissue damage by inadvertently applying excessive force to tissue. The surgeons base such crucial medical decisions on their perception and differentiation of the tissue's stiffness [4]. Stress injury from surgical forceps may result in pathological scar tissue formation, bleeding, adhesions and loss of bowel motility [5]. And organs manipulated during MIS surgery without haptic feedback that may be injured include liver, small bowel and ureter. The lack of haptic feedback is regarded as a limiting factor in existing master-slave surgical robot system [6]-[9].

Control design of such a telerobotic system with haptic feedback is challenging. Most popular bilateral control structures of practical interest are the position error based control (PEB) [10]-[13] and the direct force reflecting control (DFR) [14], [18]-[20]. In PEB control, the force or torque is applied to the motors o the haptic device, which is proportional to the position error on the slave side. This can be interpreted as a virtual spring and damper. An advantage of such control structure is that no expensive force sensor is needed, the use of the PEB control can reduce essential cost of the teleoperator. On the other hand, a number of schemes with force reflecting are based on the passivity properties, the passivity of the slave subsystem can be preserved by utilizing the PEB control [15]-[16]. However, the drawback of such system is that the human operator feels the dynamics of the slave robot. This drawback becomes more apparent if the dynamics of the slave robot is large compared to the remote contact forces, as it is the case in surgical robots with soft human tissue interaction.

To solve the aforementioned problems of PEB control, the DFR approach with a force sensor in the surgical instrument is usually favored for medical applications [18]-[20]. This control method increases the transparency of the teleoperation system. The dynamics of the slave robot is hid, and the environment contact force can be directly felt by the human operator. The drawback of such DFR control is that the system passivity is lost due the velocities and forces exchanged by the master and slave robots are not collocated. As a result, the DFR control suffers from stability problems during hard contact tasks. Furthermore, it is well known that the existence of time delay in the communication channel of a bilateral telerobotics leads to performance deterioration and causes the instability of the overall system [21]-[22]. The problem of stabilization of the force reflecting telerobotics systems in the presence of time delay is widely addressed in the literature. It is worth noting that most of the previous works address the stabilization problem in a simplified setting.

Recently, a Kalman filter, suitable for sensor noise compensating and sensor fusion, has been used extensively for a wide range of applications, such as force control of robotic manipulators [23]-[24], human-machine interface [25], and teleoperation systems [26]-[28].

This work was supported in part by the Projects of the Shanghai Science and Technology Committee under Grant 21S31906100 and 21S31903300.

Hongbing Li is with the Department of Instrument Science and Engineering, Shanghai Jiao Tong University, Shanghai, 200240 China (corresponding author to provide phone: 86-21-34207229; fax: 86-21-34205372; e-mail: lihongbing@sjtu.edu.cn).

Xun Nie with the Department of Instrument Science and Engineering, Shanghai Jiao Tong University, Shanghai, 200240 China (e-mail: tikitaka@sjtu.edu.cn)

Evgeni Magid is with the Higher Institute of Information Technology and Information Systems, Kazan Federal University, Kazan, Russia (e-mail: dr.e.magid@ieee.org).

Dingkun Gui is with Department of Nephrology, Shanghai Jiao Tong University Affiliated Sixth People's Hospital, Shanghai 200233 China (e-mail: dingkungui@sjtu.edu.cn).

In this paper, we apply a Kalman filter based approach to the problem of stable bilateral teleoperation with position error based force reflecting in the presence of time delay in both forward and backward channels. We assume that the slave robot experiences contact with the environment, which satisfies a form of passivity assumption. In the proposed algorithm, Kalman filter is incorporated to estimate both the slave robot speed and the external contact force. Experiments are carried out to show the performance of the proposed estimator.

This paper is organized as follows. First, Section II introduces the concept of speed detection and force estimation method. Then, Section III presents bilateral controller. In Section IV, experimental setup and experimental results are presented. Finally, this paper is concluded in Section V.

II. The Mechanism of Velocity and Force Estimation

A. Conventional Speed Detection Method

The incremental encoder is one of the most frequently used position transducers in robotics. The number of the generated pulses is proportional to the angular position of the shaft. The classical and probably the simplest method to measure rotor speed is the direct measure of the frequency of the encoder pulses [29]-[30]. The number of pulses is counted during a fixed sampling period, and the angular speed is then approximated to the discrete incremental ratio:

$$\omega = \frac{d\theta}{dt} \cong \frac{\Delta\theta}{T_{sc}} \cong \frac{2\pi}{N_p}\frac{\Delta N}{T_{sc}}\left[rad/s^{-1}\right] \tag{1}$$

where N_p is the number of pulses per revolution, T_{sc} is the fixed sampling period, and ΔN is the number of observed pulses inside this period.

The above method has been widely used in most telerobotics systems to measure the joint speeds from shaft encoder. However, due to the uncertainty of the measured pulse number ΔN in equation (1), there is a quantization error in the effective angular speed. A commonly adopted method to address such problem is to increase the speed sampling time and control period. However, measurement system with high sampling time leads to the bandwidth depression of system controller. Furthermore, robot joint speed is obtained with the limited speed detecting frequency due to the limited encoder pulse frequency. Especially in low speed region, in which the surgical robots most frequently perform surgery tasks, the performance of speed control is very poor.

B. Speed and Driving Current Estimation

To overcome the above mentioned problem, an observer based algorithm is developed. The state equations of the slave robot are given by

$$\frac{d\boldsymbol{X}}{dt} = \boldsymbol{A}\boldsymbol{X} + \boldsymbol{B}\boldsymbol{U} + W \tag{2}$$

$$y = \boldsymbol{H}\boldsymbol{X} \tag{3}$$

$$\boldsymbol{Z} = \boldsymbol{H}\boldsymbol{X} + V \tag{4}$$

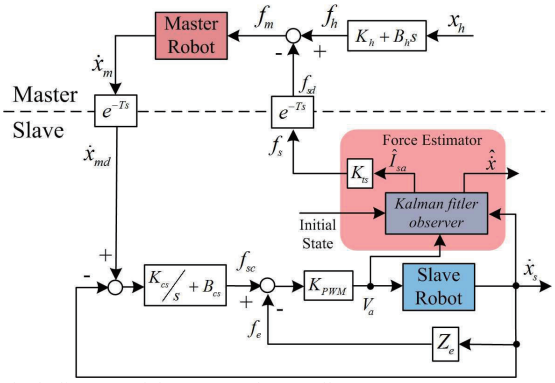

Fig.1. Block diagram of the proposed controller.

where $\boldsymbol{A} = \begin{bmatrix} -R_s/L_s & -K_{bs}/L_s \\ K_{ts}/J_s & -B_s/J_s \end{bmatrix}$, $\boldsymbol{B} = \begin{bmatrix} 1/L_s \\ 0 \end{bmatrix}$,

$$\boldsymbol{H} = [0 \quad 1], \boldsymbol{X} = [i_{sa}, \omega]^T, \tag{5}$$

where ω is the velocity of the joint shaft, L_s is the armature winding inductance of the slave robot, R_s is the armature winding resistance of the slave robot, J_s is the moment of inertia of rotor and load, B_s is the damping coefficient, K_{ts} is the motor torque constant, K_{bs} is the back emf constant.

The input here is the reference voltage u_{sa}, state variables are the mechanical angular velocity ω and the driving current i_{sa}, the output variable y is the mechanical angular velocity ω. W is the system noise and V is a measurement noise in the system modeling. Both W and V are assumed to be zero-mean white Gaussian noise inputs. The system noises come from the non-ideal current controller and the non-ideal characteristics of the driving motor. The measurement noise is driven from the imperfectness of the joint encoder and the quantization of the joint position. As a result, the variance matrix of the system noise vector $\boldsymbol{Q}$ and the variance matrix of the measurement noise vector $\boldsymbol{R}$ are written as

$$\boldsymbol{Q} = \begin{bmatrix} q_{00} & 0 \\ 0 & q_{11} \end{bmatrix}, \quad \boldsymbol{R} = [r_{00}] \tag{6}$$

where q_{00} is the voltage reference covariance value, q_{11} is the driving current covariance value, r_{00} is the measurement covariance value.

The discrete form of equation (2) is

$$\boldsymbol{X}_{k+1} = \boldsymbol{A}_k\boldsymbol{X}_k + \boldsymbol{B}_k\boldsymbol{U}_k + W_k \tag{7}$$

$$y_k = \boldsymbol{H}_k\boldsymbol{X}_k + V_k \tag{8}$$

where $\boldsymbol{A}_k$, $\boldsymbol{B}_k$, $\boldsymbol{H}_k$, W_k , V_k ,are discrete forms of system matrices. The equations for the Kalman filter fall into two groups: time update equations and measurement update equations. The time update equations are responsible for projecting forward the current states and error covariance estimates to obtain a priori estimates for the next time step. The measurement update equations are responsible for incorporating a new measurement into the a priori estimate to obtain an improved a posteriori estimate. The time update

equations can also be thought of as predictor equations and project the current state estimate ahead in time, while the measurement equations can be thought as corrector equations and adjust the projected estimate by an actual measurement at that time. The final estimation algorithm resembles that of a predictor-corrector algorithm for solving numerical problems. The specific equations for the time update and measurement update are given by

$$\bar{\boldsymbol{X}}_{k+1} = \boldsymbol{A}_k \boldsymbol{X}_k + \boldsymbol{B}_k \boldsymbol{U}_k \tag{9}$$

$$\bar{\boldsymbol{P}}_{k+1} = \boldsymbol{A}_k \boldsymbol{P}_k \boldsymbol{A}_k^{\,T} + \boldsymbol{Q}_k \tag{10}$$

The time update equations in (9) and (10) project the states and covariance estimates forward from time step $k-1$ to step k. The first task during the measurement update is to compute the Kalman gain $\boldsymbol{G}_k$, as follows

$$\boldsymbol{G}_k = \bar{\boldsymbol{P}}_k \boldsymbol{H}_k^{\,T} \left(\boldsymbol{H}_k^{\,T} \bar{\boldsymbol{P}}_k \boldsymbol{H}_k + \boldsymbol{R}_k \right)^{-1} \tag{11}$$

While the next step is to actually measure the process to obtain the input $\boldsymbol{Z}_k$, and then generate a posteriori state estimate by incorporating the measurement as

$$\hat{\boldsymbol{X}}_k = \bar{\boldsymbol{X}}_k + \boldsymbol{G}_k \left[\boldsymbol{Z}_k - \left(\boldsymbol{H}_k \bar{\boldsymbol{X}}_k \right) \right] \tag{12}$$

The final step is to obtain a posteriori error covariance estimates through the following equation,

$$\boldsymbol{P}_k = \left(I - \boldsymbol{G}_k \boldsymbol{H}_k \right) \bar{\boldsymbol{P}}_k \tag{13}$$

After each time and measurement update pair, the process is repeated with the previous a posteriori estimates used to project or predict the new a priori estimates. This recursive nature is one of the very appealing features of the Kalman filter.

C. External Force Estimation

The estimation of external contact force at slave side can be accomplished by means of modeling the slave robot dynamics. The slave robot dynamics and the relationship between force and torque on the end effector is described by the following equations,

$$f_s = M_s \ddot{x}_s + B_s \dot{x}_s + C_s + f_f + f_{ext} \tag{14}$$

where f_s is the vector of motor torque exerted in slave robot joint, f_{ext} is the vector of force ejected in the robot end effector, M_s is the slave robot inertia matrix, B_s is the damping coefficient, C_s is the gravity force vector, f_f is the friction torque vector, f_{ext} is the external force on the joint. By combining (19) and (20), the external contact forces at the slave robot tip result on

$$f_{ext} = f_s - M_s \ddot{x}_s + B_s \dot{x}_s + C_s + f_f \tag{15}$$

Since general minimally invasive surgery is characterized by slow motions (0-2Hz) [31], the dynamic effect of the end-effector $M_s \dot{\omega}_s$ is assumed to be minimal. With appropriate handling of the friction in the power transmission mechanism, the friction effect can also be assumed to be relatively small. The gravity term C_s can also be compensated in the controller.

For the surgical robot with light weight, low friction and backdrivable capability, it is believed that the torque required to overcome the external contact force on the instrument tip can be estimated from the driving current of the joint motor. Based on the theory of the servo motor and the current amplitude, the driving current of the joint motor is linear proportional to its output torque,

$$\tau_s = K_{ts} i_{sa} \tag{16}$$

As a result, it is possible to determine the external contact forces excreted on the robot tip.

$$f_{ext} = \left(J^T \right)^{-1} \tau_s \tag{17}$$

III. Designing of the Bilateral Controller

A. Design Optimization for Enhanced Force Sensation

To provide the sensor of touch, robot in master-slave configurations has been proposed. The concept of bilateral control is made on the basis of the exchanged information between the driving actuators. The bilateral control supplies force feedback information to the human operator through a master robot. On the other hand, a slave robot is applied to interact with unknown environment. During fine manipulation within a surgical procedure, contact force information of an environment is perceived through the human kinaesthesia. Reliable transmission of the contact force signal through the teleoperator system, restoring the surgeon's ability to differentiate during surgical procedures, is presented as the optimization goal for the control design of the teleoperation system.

Controllers are optimized for operator force perception abilities rather than for traditional teleoperation goals of motion tracking or force feedback fidelity. Thus, the target of the ideal bilateral control is to minimize the difference between the force responses in the master and slave side as follows:

$$f_{ext}^{m} = f_{ext}^{s} \tag{18}$$

Moreover, the position tracking of the master and slave robots should be similar, as follows:

$$x_m = x_s \tag{19}$$

B. Bilateral Controller

For simplicity, both master and slave robots are one degree-of-freedom devices and can be modeled by the following linear dynamics.

master: $f_m(t) = M_m \ddot{x}_m(t) + B_m \dot{x}_m(t)$ (20)

slave: $f_{sc}(t) = M_s \ddot{x}_s(t) + B_s \dot{x}_s(t)$ (21)

where M_m, B_m and x_m are the manipulator's inertia, damping coefficient and displacement, respectively, ($i = m, s$ indicates the master, m or slave, s, manipulator). The forces f_m and f_{sc} applied to the manipulators depend both on the interaction with the operator/environment and on the control action. In general, these forces can be defined as

$$f_m = f_h - f_{sd}\,,\; f_{sc} = f_s - f_e \tag{22}$$

where f_h, f_e are the forces imposed by the human operator and by the environment, respectively. f_s is the force computed by the control algorithms as equation (17).

$$f_s = f_{ext} \tag{23}$$

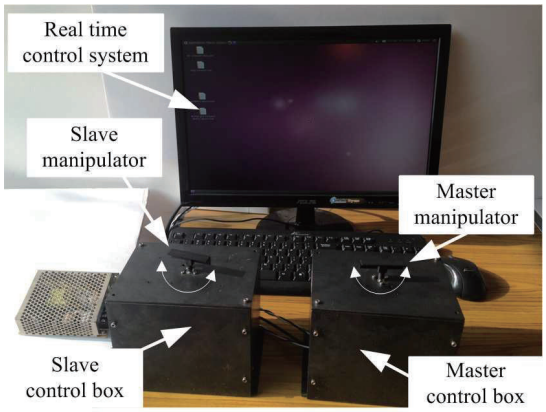

Fig.2. Experiment setup of 1 DOF teleoperation system.

From the master slave system model, the block diagram of the controller can be shown in Fig.1. As there is no force sensor at the master manipulator, the manipulating force of operator is calculated by a linear impedance model which is given as

$$f_h = K_h(x_h - x_m) + B_h(\dot{x}_h - \dot{x}_m) \quad (24)$$

where K_h and B_h are impedance matrixes of the stiffness and damping.

IV. Experimental Results

A. Experimental Setup

The setup consists of two identical 1-DOF devices powered by DC motors without a gearbox, as shown in Fig.2. The DC motor used in this experiment is made by Maxon, Switzerland which is driven by a PWM Amplifier (Maxon ADS 50-5). The model number of the motor is RE 25. A real time Linux OS was installed at the PC to maintain an accurate sample interval. An optical encoder (MEH-12-1000P, Microtech Laboratory Inc.) is mounted at the motor axis for sensing the rotational motion of the handle. Both devices are controlled from the same controller running a real time Linux distribution. The time delay is emulated using a buffering algorithm. The master slave device parameters and control parameters are shown in Table I. During all the experiments, the master device was manipulated by human hand and the slave robot is driven to contact with phantom human tissue.

TABLE I
PARAMETERS FOR EXPERIMENT

Parameters	Quantity	Value
M_m	mass of the master device	0.01 kg
B_m	viscosity of the master device	0.01 Ns/mm
M_s	mass of the master device	0.01 kg
B_s	viscosity of the master device	0.01 Ns/mm
K_m	proportional control gain on master side	0.25 N/mm
K_s	proportional control gain on slave side	0.25 N/mm
B_s	derivative control gain on slave side	0.031 Ns/m
K_{st}	Torque constant	0.044Nm/A

B. Experimental Results

In this section, we report, compare, and discuss the results obtained from the experiments that we have conducted on the proposed controllers. Firstly, we performed a series of experiments using a real master slave teleoperation device, assuming the time delay in the communication line is very small. Secondly, we performed experiments considering the longer time delay in the signal transmission line. In both cases, the hypothetical slave system consisted of a single axis robot with a linear stiffness as the task environment.

1) Tracking in Contact Motion with Small Time Delay

We firstly assume that there is a small time delay (round time delay100ms) between the master and slave robot stations and the proposed force sensorless contact force estimation algorithm is applied to the controller. The slave robot was driven by the master robot manipulating by human operator to contact the phantom tissue several times and the experimental results are shown in Fig.3.

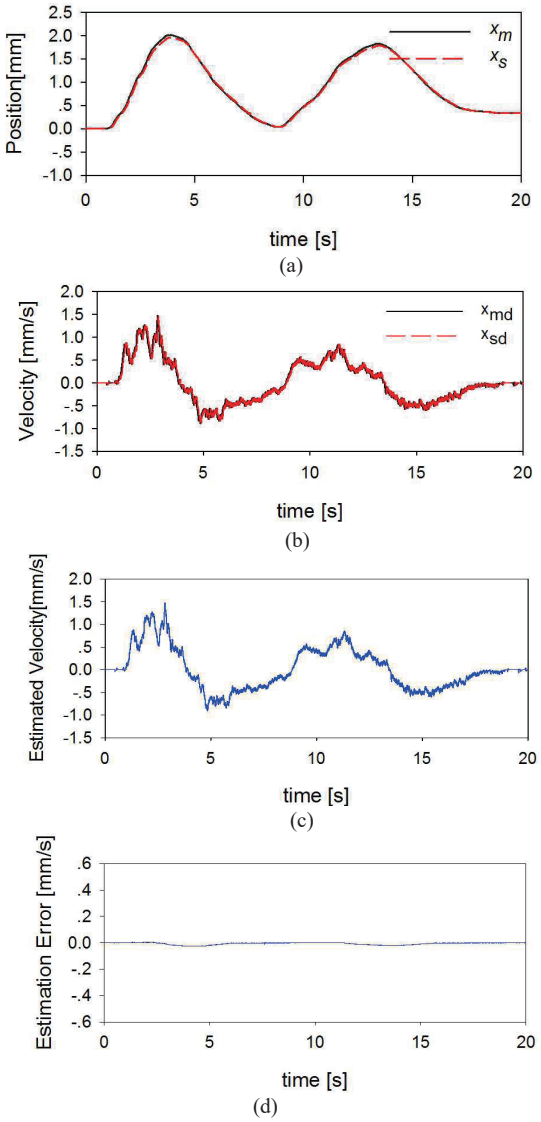

Fig.3. System performance under round time delay 100ms. (a) master slave robot position tracking, (b) master slave robot velocity tracking, (c) the estimated velocity by Kalman filter, (d) velocity estimation error.

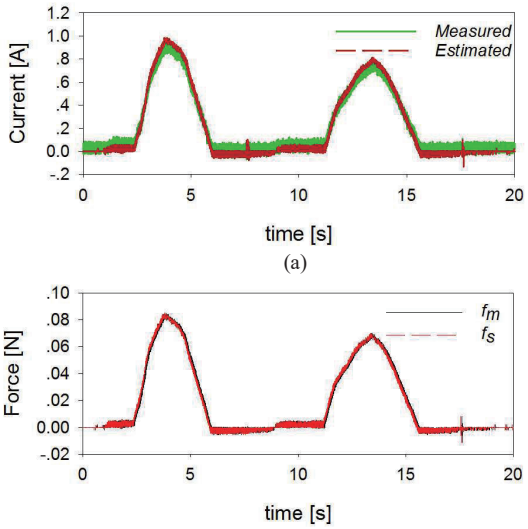

Fig.4.The estimated and measured current (a) and force (b) under round time delay100ms.

The position responses of the master and slave manipulators show stable interaction (Fig.3 a). Figure 3 b shows the velocity tracking performance during the experiments. The slave robot velocity follows the reference master robot velocity very well. Both of the master and slave robots velocities are calculated from the position information with the output signal of optical encoders. The estimated velocity on slave side is shown by Fig.3 c. Compared with the calculated velocity from optical encoder, the velocity estimation error is small than ± 0.1mm/s. Such error between the state value of velocity estimation and velocity calculation is used to characterize the accuracy of the proposed method. Figure 4 shows the result by comparing the current estimations with the respective current measurement for current sensor. It is noticed that the current estimation has some noise at the free motion period, due to dynamic effects. The current prediction error is small except when the position changes its direction, as it is expected due the uncertainty of the friction at free motion. The estimated current in dashed red line of Figure 4 is then used to calculate the feedback force to the master robot.

2) Tracking in Contact Motion with Larger Time Delay

In order to check the system performance of the proposed approach for a longer time delay in the communication line, a similar experiment was carried out with the same experimental conditions as the above experiment. Here, the round time delay in the communication line is set as 200ms. Figure 5 and 6 show the experimental results. Similar to the previous experimental results shown in Fig.3 and 4, the position response of the master and slave were sta ble (Fig.5 a). The stable performance of the force at master side and the contacting force from the external environment are shown in Fig.6 b. The feedback force to the master side is calculated from the estimated driving current of the motor driver. The minimal velocity error between the estimated and calculated one validates the effectiveness of the proposed control method (Fig. 6 a). The repeated testing results demonstrate that the performance of this external force estimation method is relatively robust.

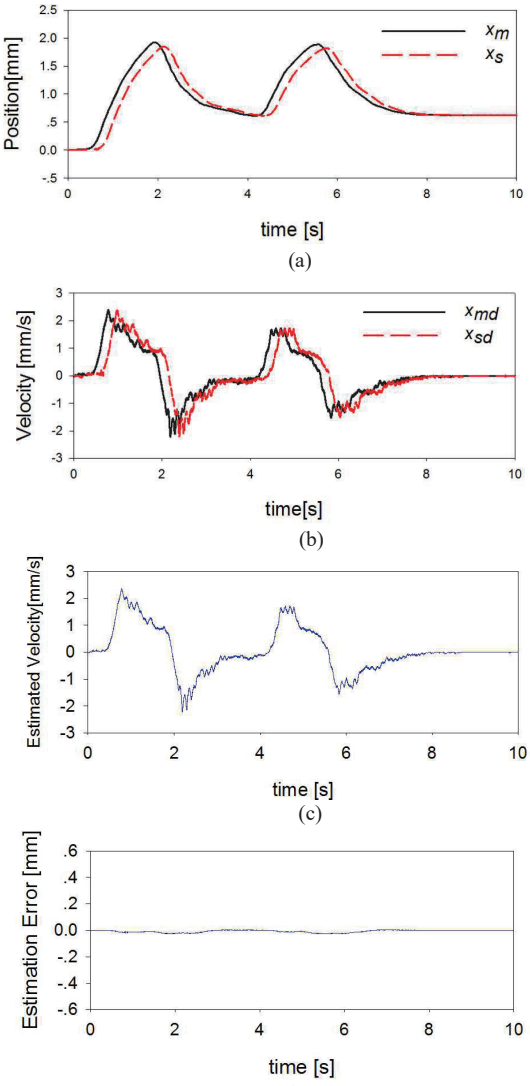

Fig.5. System performance under round time delay 160ms. (a) master slave robot position tracking, (b) master slave robot velocity tracking, (c) the estimated velocity by Kalman filter, (d) velocity estimation error.

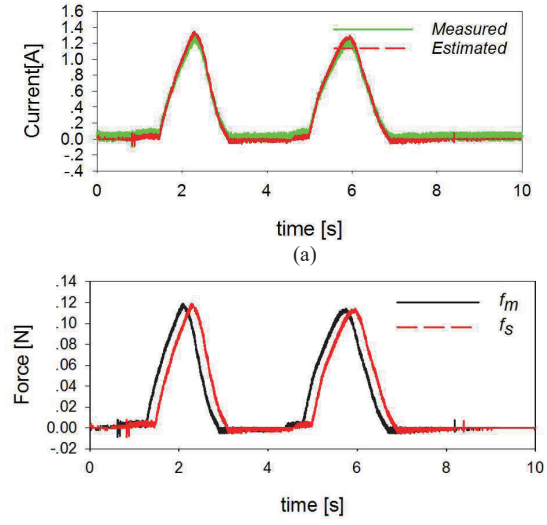

Fig.6.The estimated and measured current (a) and force (b) under round time delay 200ms.

V. Conclusion and Future Works

This paper describes a novel approach to estimate slave side driving current and velocity of a delayed teleopration system based on Kalman filter. The external contact force ofon the slave side robot is calculated based on the estimated driving current. Experimental results show that stable trajectory tracking is achieved while the remote slave contact force is accurately displayed to the human operator. Thus a high transparency of the master slave teleoperation system is achieved. The greatest advantage of this method is that it requires no force/torque sensors installed at the slave side robot.

To improve the performance of the proposed approach further, future development will be conducted on the following aspects. Firstly, the external force calculated from the current of the driving motor includes the motor effort to compensate the operating force together with the robot mechanical dynamics. This will cause some estimation errors when the robot mechanism becomes more complex. Secondly, since in the long term we aim to achieve reliable telesurgery under the commonly used networks, the general nonlinear teleoperation system with packet loss and chattering time delay should be modeled in designing of the system controller. Moreover, experiments utilizing master slave robots with multiple degrees of freedom have to be conducted in the future.

References

[1] G.S.Guthart and J.K.Salisbury, "The intuitive telesurgery system: Overview and application," in *IEEE* International Conference on Robotics and Automation, pp.618-621, 2000.

[2] D.Zhao, L.Ma, C.Ma, J.Tang,H.Tang, "Floating autostereoscopic 3D display with multidimensional images for telesurgical visualization," International Journal of Computer Assisted Radiology and Surgery, Vol.11, No.2, pp.207-215, 2016.

[3] K.Deary, A.Melzer, V.Watson, G.Kronreif, and D.Stoianovici, "Interventional robotic systems: Applications and technology state-of-theart," Minimally Invasive Therapy, vol.15, pp.101-113, 2006.

[4] P.Puangmali, K.Althoefer, L.D.Seneviratne, D.Murphy, and P.Dasgupta, "State-of-the-art in Force and Tactile Sensing for Minimally Invasive Surgery," *IEEE* Sensors Journal, vol.8, pp.371-381, 2008.

[5] S.De, J.Rosen, A.Dagan, B.Hannaford, P.Swanson, M.Sinanan, "Assessment of tissue damage due to mechanical stresses," International Journal of Robotics Research, Vol.26, No.11, pp.1159-1171, 2007.

[6] B.Zhao, C.A.Nelson, "Sensorless force sensing for minimally invasive surgery," ASME Journal of Medical Devices, Vol.9, pp.041012-1-14, 2015.

[7] M.Haghighipaanh, M.Miyasaka, and B.Hannaford, "Utilizing elasticity of cable driven surgical robot to estimate cable tension and external force," *IEEE* Robotics and Automation Letters, Preprint, 2017.

[8] D.-H. Lee, U.Kim, T.Gulrez, W.J.Yoon, B.Hannaford, "A laparoscopic grasping tool with force sensing capability," *IEEE/ASME* Transactions on Mechatronics, vo.21, no.1, pp.130-141, 2016.

[9] U.Kim, D.-H.Lee, Y.B. Kim, D.-Y.Seok, J.So,and H.R.Choi, "S-Surge: Novel portable surgical robot with multi-axis force-sensing capability for minimally invasive surgery," *IEEE/ASME* Transactions on Mechatronics, Early view on line , pp.1-11, 2017.

[10] I.G.Polushin, P.X.Liu, C.Lung, G.D.On, "Position-error based schemes for bilateral teleoperation with time delay: Theory and experiments," ASME Journal of Dynamic Systems, Measurement, and Control, Vol.132, pp.031008-1-11, 2010.

[11] H.Li, K.Kawashima,"Experimental comparison of backdrivability for time-delayed telerobotics," Control Engineering Practice, Vol.28, pp.90-96, 2014.

[12] H.Li, K.Tadano, and K.Kawashima, "Experimental validation of stability and performance for position error based tele-surgery," *IEEE/ASME* International Conference on Advanced Intelligent Mechatronics, pp.848-853, Busan, South Korea, July 07-11, 2015.

[13] R.Uddin, S.Park, adn J.Ryu, "A predictive energy-bounding approach for haptic teleoperation," Mechatronics, Vol.35, pp.148-161, 2016.

[14] M.Franken, S,Stramigioli, S.Misra, C.Secchhi, A.Macchelli, "Bilateral telemanipulation with time delays: A two-layer approach combining passivity and transparency," *IEEE* Transactions on Robotics, Vol.27, No.4, pp.741-756, 2011.

[15] A.Jazayeri, M.Tavakoli,"Bilateral teleoperation system stability with non-passive and strictly passive operator or environment," Control Engineering Practice, Vol.40, pp.45-60, 2015.

[16] R.J.Anderson, M.W.Spong,"Bilateral control of teleoperators with time delay," *IEEE* Transactions on Automatic Control, Vol.34, No.5, pp.494-501, 1989.

[17] H.Li, K.Kawashima,"Bilateral teleoperation with delayed force feedback using time domain passivity control," Robotics and Computer-Integrated Manufacturing, Vol.37, pp.188-196, 2016.

[18] A.Okamura. "Methods for haptic feedback in teleoperated robotassisted surgery," In Industrial Robot: An international Journal, Vol.31, No.6, pp.499-508, 2004.

[19] H.Liu, M.Selvaggio, P.Ferrentino, et al.,"The MUSHA hand II: A multifunctional hand for robot-assisted laparoscopic surgery," *IEEE/ASME* Transactions on Mechatronics, Vol.26, No.1, pp.393-404, 2021.

[20] T.Li, A.Pan, and H.Ren, "Reaction force mapping by 3-axis tactile sensing with arbitrary angles for tissue hard-inclusion localization," *IEEE* Transactions on Biomedical Engineering, Vol.68, No.1, pp.26-35, 2021.

[21] R.Bavili, A.Akbari, R.Esfanjani,"Control of teleoperation systems in the presence of varying transmission delay, non-passive interaction forces, and model uncertainty," Robotica, Vol.39, No.8, pp.1451-1467, 2021.

[22] H.Li, and K.Kawashima, Achieving stable tracking in wave-variable based teleoperation, *IEEE/ASME* Transactions on Mechatronics, Vol.19, No.5, pp.1574-1582, 2014.

[23] V.Agarwal,and H.Parthasarathy,"Disturbance estimator as a state observer with extended Kalman filter for robotic manipulator," Nonlinear Dynamics, Vol.85, No.4, pp.2809-2825, 2016.

[24] F.Cao, P.D.Docherty,S.Ni, X.Chen,"Contact force and torque sensing for serial manipulator based on an adaptive Kalman filter with variable time period," *Robotics and Computer-Integrated Manufacturing*,Vol.72, pp.102210, 2021.

[25] Q.Wu, and Y.Chen, "Development of an intention-based adaptive neural cooperative control strategy for upper-limb robotic rehabilitation," *IEEE* Robotics and Automation Letters, Vol.6, No.2, pp.335-342, 2021.

[26] M.C.Cavusoglu, and F.Tendick, "Kalman filter analysis for quantitative comparison of sensory schemes in bilateral teleoperation systems," *IEEE* International Conference on Robotics and Automation, Vol.2, pp.2818-2823, 2003.

[27] R.Cortesao, J.Park, and O.Khatib, "Real-time adaptive control for haptic telemanipulation with Kalman active observers," *IEEE* Transactions on Robotics, Vol.22, No.5, pp.987-999, 2006.

[28] C.Mitsantisuk, K. Ohishi, and S.Katsura, "Estimation of action/reaction forces for the bilateral control using Kalman filter," *IEEE* Transactions on Industrial Electronics, Vol.59, No.11, pp.4383-4393, 2012.

[29] T.Ohmae et al. "A microprocessor-controlled high-accuracy wide-range speed regulator for motor drives," *IEEE* Transactions Industrial Electronics, Vol.IE-29, No.3, 1982.

[30] R.Petrella, M.Tursini, L.Peretti,M.Zigliotto, "Speed measurement algorithms for low-resolution incremental encoder equipped drives: a comparative analysis," International Aegean Conference on Electrical Machines and Power Electronics,Sep.10-12, 2007.

[31] B.Hannaford, Experimental measurements for specification of surgical mechanisms and understanding of surgical skill, Lecture Notes of the European Summer School on Surgical Robotics, Montpellier, France, September, 2003.